Electronic Supplementary Material (ESI) for Physical Chemistry Chemical Physics.

Supporting information for: Loss channels in Triplet-Triplet Annihilation Photon Upconversion: Importance of Singlet and Triplet Surface Shapes

Victor Gray,[†] Ambra Dreos,[†] Paul Erhart,[‡] Bo Albinsson,[†] Kasper Moth-Poulsen,[†] and Maria Abrahamsson[*,†]

Department of Chemistry and Chemical Engineering, Chalmers University of Technology, Gothenburg, Sweden, and Department of Physics, Chalmers University of Technology, Gothenburg, Sweden

E-mail: abmaria@chalmers.se

---

[*] To whom correspondence should be addressed

[†] Department of Chemistry and Chemical Engineering, Chalmers University of Technology, Gothenburg, Sweden

[‡] Department of Physics, Chalmers University of Technology, Gothenburg, Sweden

Contents

1 Triplet-Triplet Annihilation Upconversion Mechanism

The sensitizer absorbs a photon promoting it to its first excited singlet state followed by inter-system crossing (ISC) to the first triplet excited state. The triplet state of the annihilator is then populated through triplet energy transfer (TET) from the sensitizer. Two triplet excited annihilators then interact and annihilate forming a singlet excited annihilator and one ground state annihilator. The singlet excited annihilator can finally return to its ground state through fluorescence, emitting a photon. The energy transfer processes involved are schematically described in the Jablonski diagram in Figure S1.

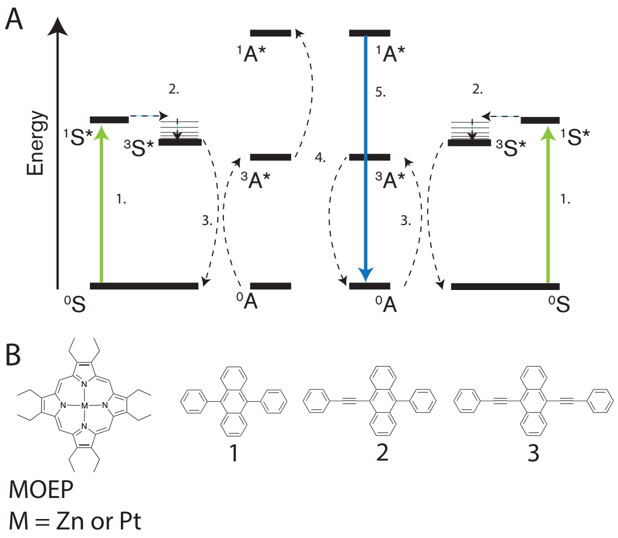

Figure S1: a) Jablonski diagram explaining the triplet-triplet annihilation upconversion process. A sensitizer absorbs a low energy photon (1) and rapidly populates its first triplet excited state after intersystem crossing (ISC) from the singlet state (2). The annihilator is sensitized through a triplet energy transfer (TET) process (3) together with the sensitizer. Two triplet excited annihilator molecules can come together whereupon they can undergo triplet-triplet annihilation (4) generating one singlet excited annihilator which can deactivate to its ground state by emitting a photon (5). b) Molecular structures of the sensitizers ZnOEP and PtOEP and the studied annihilators **1-3**.

2 Synthesis

2.1 General Information

Starting material for the synthesis, solvents, **1** and **3** were purchased from Sigma-Aldrich or Fischer Scientific. 9-bromo-10-phenylanthracene was prepared as reported previously.[S1] Dry and degassed solvents were obtained from a M-Braun solvent drying system. NMR was run on a 400 MHz Varian NMR and IR was run on a Perkin Elmer ATR-FTIR. Column chromatography was carried out using a Biotage Flash Column Chromatography system with Biotage prepacked SNAP columns. Melting points were determined using an automatic Mettler Toledo MP70 melting point apparatus.

2.2 Synthesis of 9-phenyl-10-(phenylethynyl)anthracene, 2

The title compound was prepared from the Sonogashira cross coupling of 9-bromo-10-phenylantrhacene and phenylacetylene. The solid 9-bromo-10-phenylantrhacene (800 mg, 2.4 mmol) was added together with the catalysts Pd(PPh$_3$)$_4$ (95 mg, 0.08 mmol, 3%) and CuI (18 mg, 0.1 mmol, 4%) to an oven dried reaction vessel. The atmosphere was exchanged with N_2 three times. Thereafter 11 ml dry and degassed THF was added together with 11 ml N_2 purged diisopropylamine. Phenylacetylene (0.29 ml, 2.6 mmol) was added and the mixture was purged with N_2 for 10 minutes before it was heated for reflux for 18 h. The crude was extracted with DCM and water, washed with brine and dried over Na_2SO_4. The product was purified on silica gel chromatography eluting with hexane (R_f = 0.2) followed by recrystallization of the yellow fraction to obtain 0.61 g of yellow crystals (1.72 mmol, 71%). Mp = 276.9°C. Elem. Anal.: Calc. ($C_{28}H_{18}$): C:94.88 %, H:5.12 %, Found: C:94.90 % H:5.06 %. FT-IR (ATR) $\nu(cm^{-1})$ = 3078 (m), 3058 (m), 3033 (m), 3019 (m), 1620 (w), 1696 (m), 1571 (m), 1516 (m), 1492 (m), 1478 (m), 1440 (s), 1392 (s), 1325 (w), 1275 (w), 1191 (m), 1173 (m), 1145 (m), 1109 (w), 1068 (s), 1024 (s), 999 (w), 955 (w), 924(m), 909 (m), 843 (w), 765 (s), 750 (s), 691 (s), 638 (s), 650 (s), 617 (s), 530 (s), 513 (m), 502 (m), 472 (m), 415 (s). H^1-NMR (400 MHz, $CDCl_3$) δ = 8.73 (dt, J_1 = 1.2 Hz, J_2 = 8.7 Hz, 2H) 7.81-7.77 (m, 2H), 7.66 (dt, J_1 = 1.1 Hz, J_2 = 8.8 Hz, 2H), 7.60-7.53 (m, 5H), 7.48-7.35 (m, 7H) ppm. C^{13}-NMR (400 MHz, $CDCl_3$) δ = 138.48, 138.36, 132.23, 131.63, 131.11, 129.90, 128.51, 128.44, 128.34, 127.62, 127.36, 126.86, 126.27, 125.55, 123.67, 117.40, 100.90, 86.50 ppm.

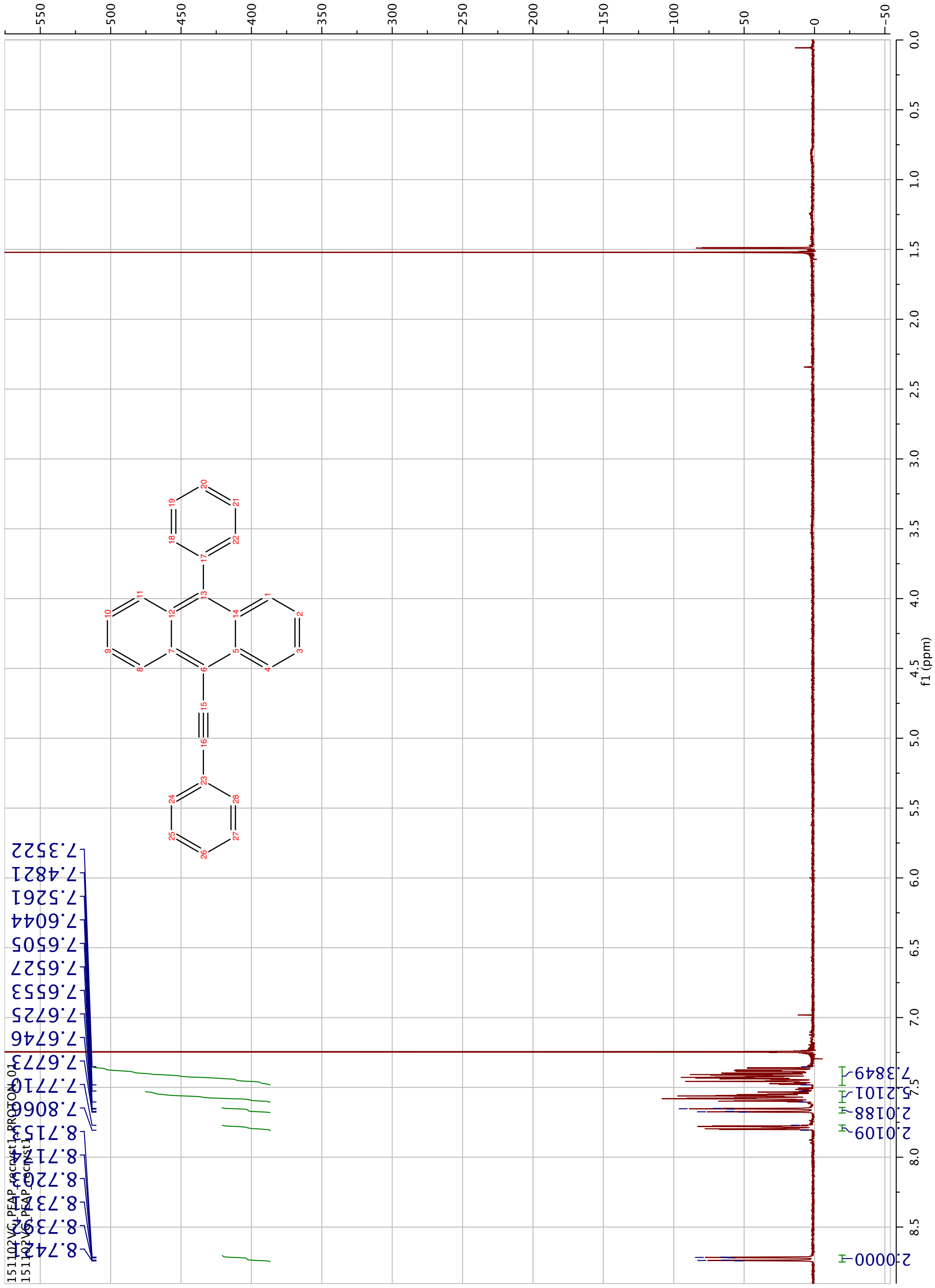

Figure S2: ^{1}H-NMR of **2**

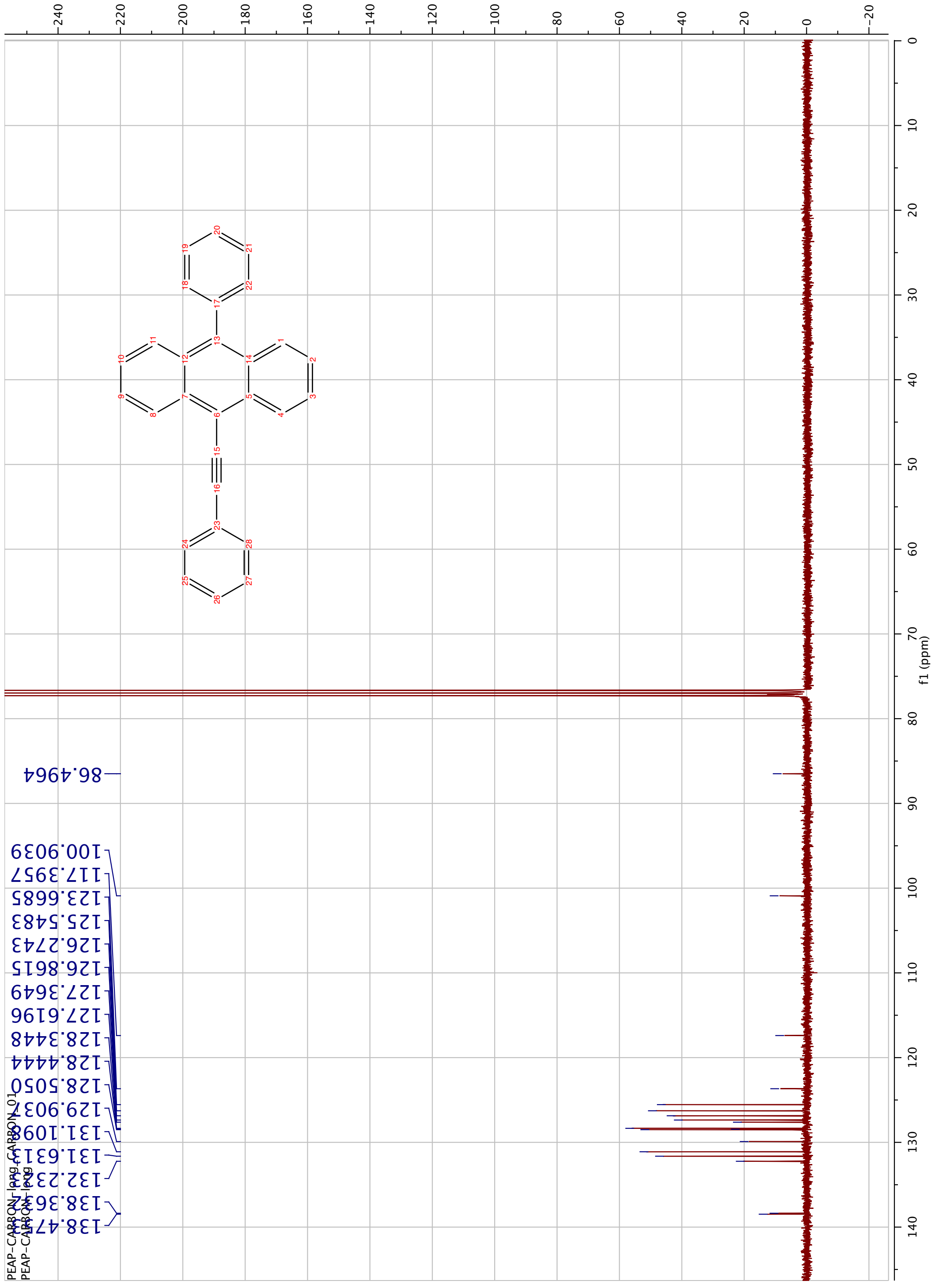

Figure S3: ^{13}C-NMR of **2**

3 Spectroscopic Measurements

3.1 General Information

Steady-state absorption was recorded on a Cary 4000 Spectrophotometer and steady state fluorescence measurements were carried out on a Spex Flurolog 3 spectrofluorimeter (JY Horiba). Fluorescence lifetimes were determined on a time correlated single photon counting (TCSPC) setup using a 377 nm laser diode (PicoQuant) and a PMT detector (10000 counts, 4096 channels). Nanosecond transient absorptions measurements were performed on home built system with a Surelite Continuum Nd:YAG laser equipped with an OPO generating a 7 ns pump beam. A quartz-halogen lamp with a monochromator was used as the probe light and a monochromator together with a 5 stage PMT coupled to an oscilloscope was used for recording the transient. Triplet lifetimes were determined in dilute samples under low pump energies to ensure that no triplet-triplet annihilation occurred.

All photophysical measurements were carried out in toluene using quartz cuvettes. Degassed samples for Stern-Volmer quenching studies and nanosecond transient absorption studies were prepared in a glovebox from Innovative Technologies (<0.1 ppm oxygen level) under nitrogen atmosphere.

Fluorescence quantum yield of **2** and **3** in toluene were determined by relative actinometry employing **3** in cyclohexane (Φ_r=100 %) as the standard using dilute solutions.[S2]

3.2 Photophysical Characterization

In table S1 the quantum yield and the fluorescence lifetime of the annihilators in this study are listed.

Table S1: Quantum yield and fluorescence lifetimes

Entry	Φ_{AF}(%)	τ_T (ns)
1	100[S1]	6.96[S3]
2	79±6[a]	3.65
3	85±1[a]	2.80

[a] average of two independent measurements and error is reported as standard deviation

3.3 Stern-Volmer Quenching of ZnOEP and PtOEP

The lifetime of the triplet state of ZnOEP was determined to 117 μs, using nanosecond time-resolved transient absorption. Samples were prepared with 8.7 μM ZnOEP and 0-60 μM annihilator. No self-annihilation was observed for ZnOEP at these low concentrations and excitation energies. Three transients at 570 nm, corresponding to the ground state bleach, were recorded with different time-windows and these were then globally fit to mono- or bi-exponential decays to yield the lifetime. Samples with only ZnOEP and ZnOEP with **2** showed only mono-exponential behavior. ZnOEP with **1** or **3** displayed bi-exponential decays as the reabsorption of the upconverted emission resulted in a delayed excitation of the ZnOEP resulting in an additional decay component. The shorter lifetime of the two was used for the Stern-Volmer fitting according to the Stern-Volmer relationship described in Equation S1. The resulting Stern-Volmer plots are shown in figure S4.

$$\frac{\tau_0}{\tau} = \frac{I_0}{I} = 1 + k_{TET}\tau_0[A] \tag{S1}$$

where τ and τ_0 are the lifetimes of the quenched and unquenched sensitizer respectively. Similarly I and I_0 are the quenched and unquenched emission intensity of the sensitizer, respectively. k_{TET} is the rate constant of triplet energy transfer and $[A]$ is the annihilator concentration. For PtOEP the quenching of the phosphorescence was used for the Stern-Volmer analysis. Samples of 0.5 μM PtOEP were prepared with 0-60 μM annihilator. The Stern-Volmer plots are compared to ZnOEP in figure S4. The lifetime of the unquenched PtOEP triplet state was determined to 91 μs on a Cary Eclipse spectrofluorometer.

The TET efficiencies were calculated from Equation S2, using using k_{TET} values determined in the Stern Volmer quenching experiments S2

$$\Phi_{TET} = 1 - \frac{\tau}{\tau_0} = 1 - \frac{1}{1 + k_{TET}\tau_0[A]} \tag{S2}$$

Figure S5 shows the estimated TET efficiency as a function of annihilator concentration for the three annihilators.

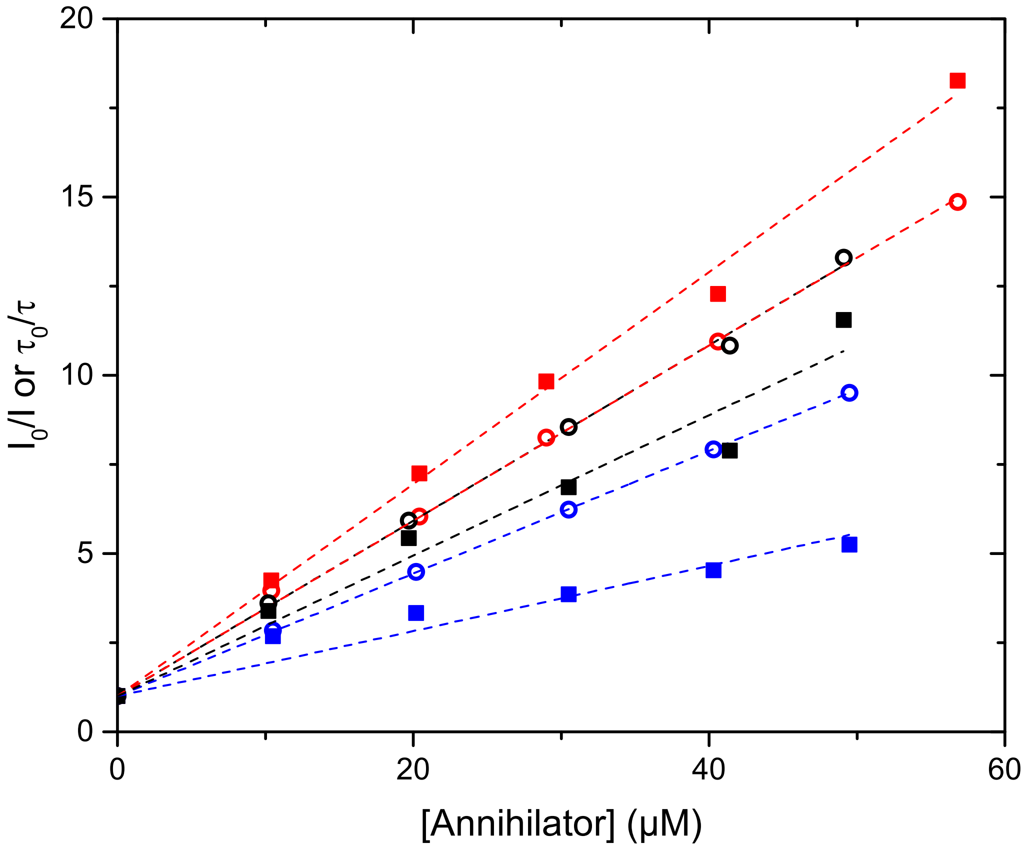

Figure S4: Stern-Volmer quenching of ZnOEP (filled) and PtOEP (open) with **1** (blue), **2** (black) and **3** (red)

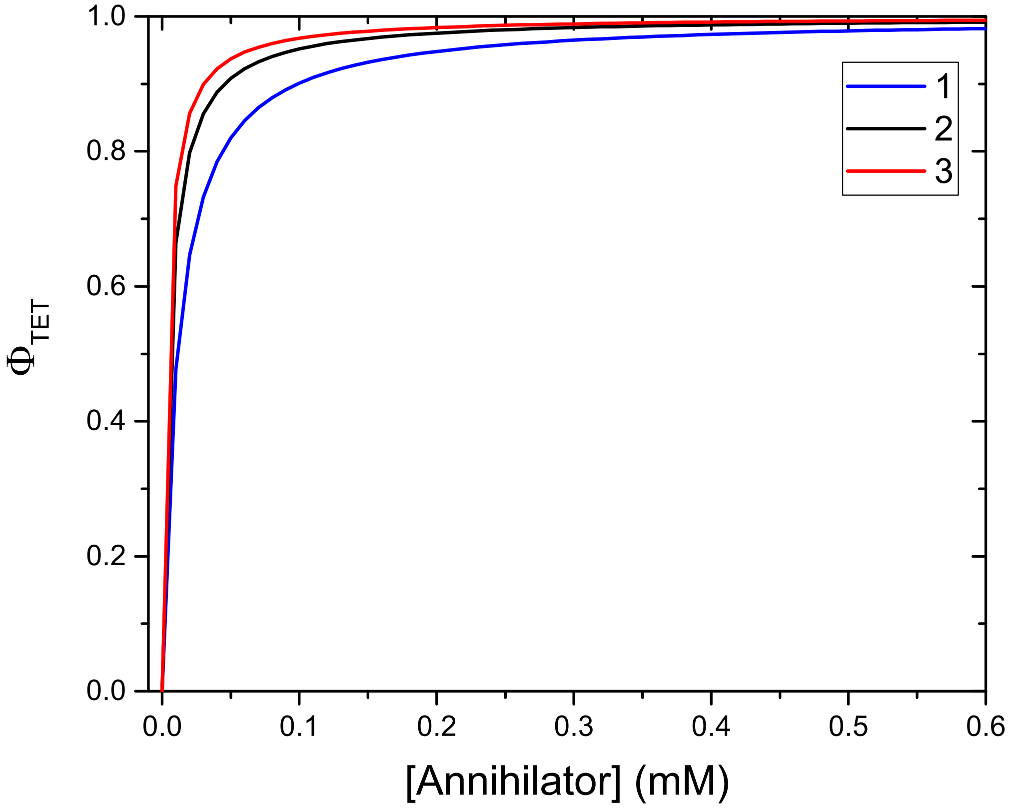

Figure S5: Estimated triplet energy transfer efficiency Φ_{TET} of ZnOEP at different annihilator concentrations, **1** (blue), **2** (black) and **3** (red)

4 Transient absorption measurements

4.1 Triplet State Lifetimes

The triplet lifetimes of **2** and **3** were determined by transient absorption measurements, monitoring the triplet excited state at 490 nm after exciting the sensitizer at 532 nm. **2** and **3** were prepared in degassed toluene (10 μM) in a glovebox and sensitized by PtOEP (0.5 μM). Concentrations and laser power were chosen to ensure no triplet-triplet annihilation would occur. To study the effect of the sensitizer concentration on the annihilator triplet lifetime the triplet lifetime of **2** was determined at low (0.5 μM) and high (50 μM) concentrations of either ZnOEP or PtOEP. The lifetime of **2** was determined to 2.41±0.12 ms when sensitized by 0.5 μM PtOEP, similarly **3** was determined to 0.5±0.03 ms. At higher PtOEP concentrations the lifetime of **2** was decreased to 1.84±0.08 ms. To compare the lifetimes determined in presence of ZnOEP were 2.02±0.16 ms and 0.68±0.03 ms for 0.5 and 50μM ZnOEP respectively.

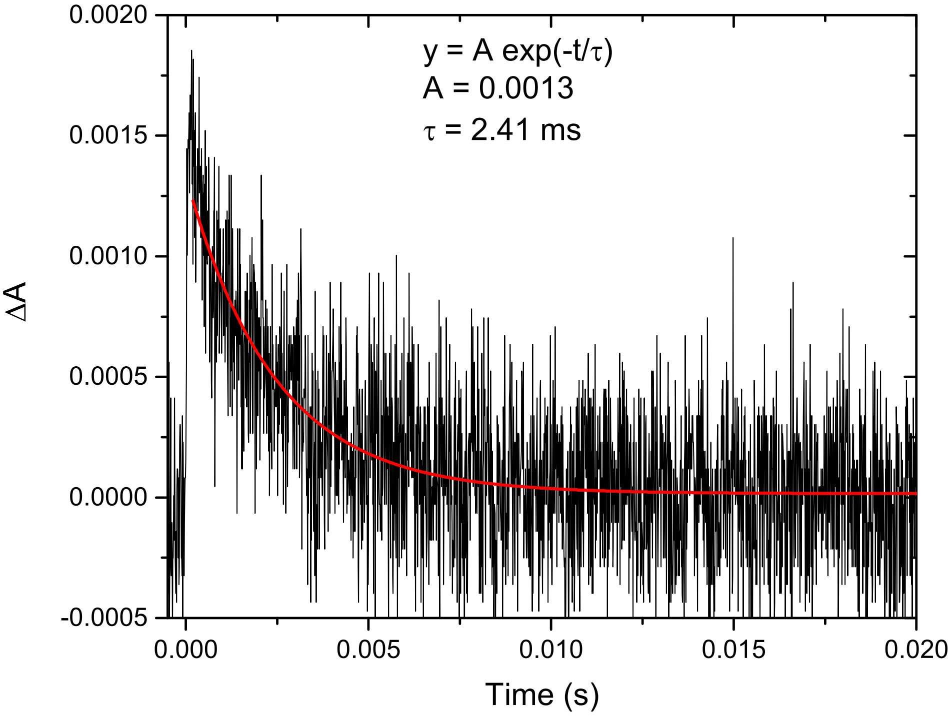

Figure S6: Transient absorption of **2** (10 μM) at 490 nm corresponding to the triplet absorption after sensitization by PtOEP 0.5 μM (black) and fitted monoexponential decay (red).

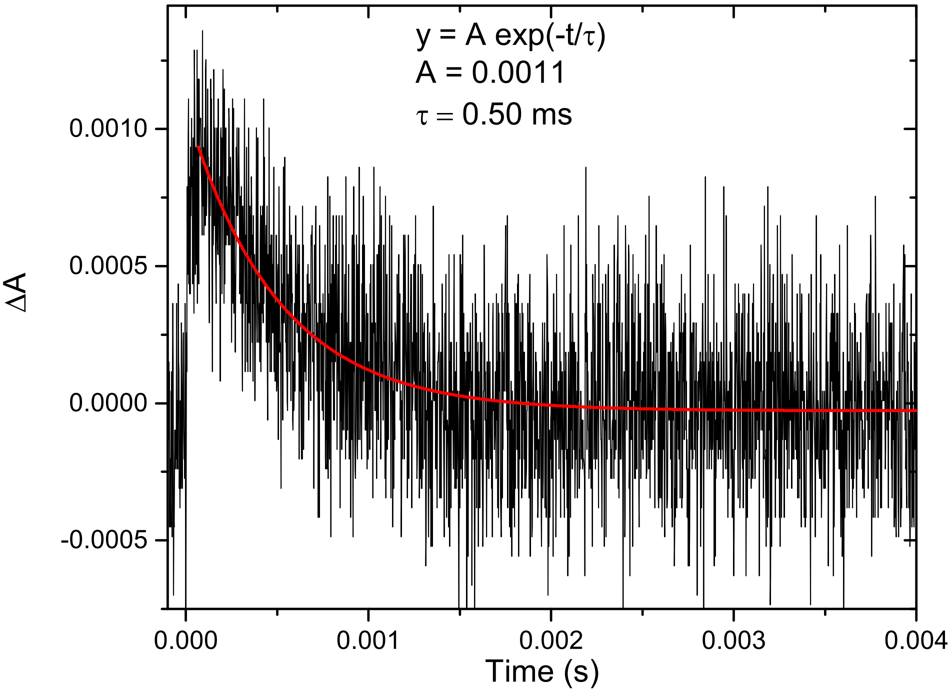

Figure S7: Transient absorption of **3** (10 μM) at 490 nm corresponding to the triplet absorption after sensitization by PtOEP 0.5 μM (black) and fitted monoexponential decay (red).

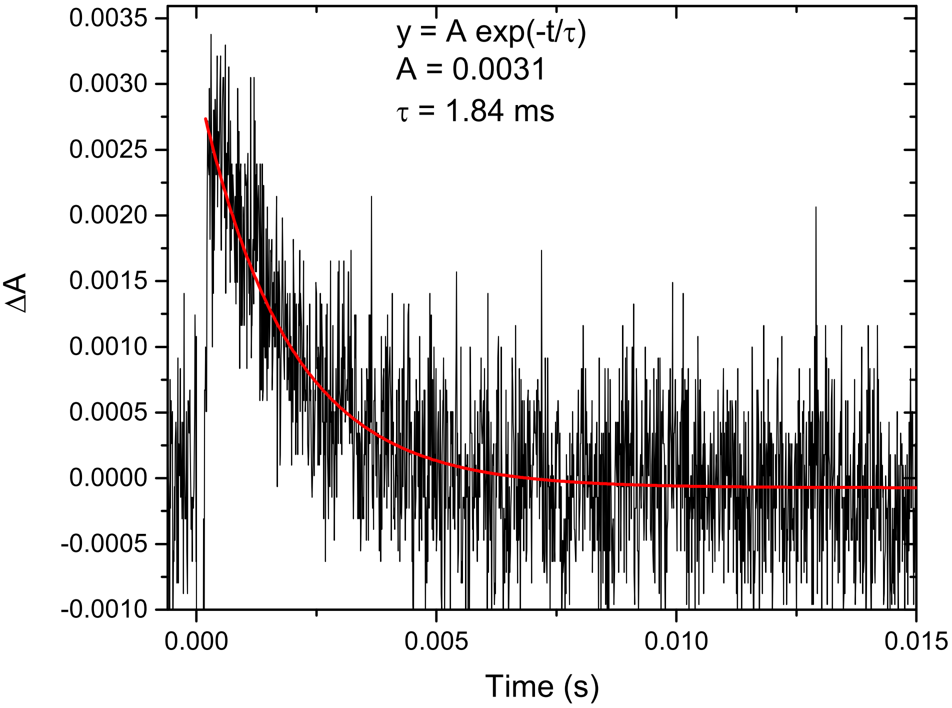

Figure S8: Transient absorption of **2** (10 μM) at 490 nm corresponding to the triplet absorption after sensitization by PtOEP 50 μM (black) and fitted monoexponential decay (red).

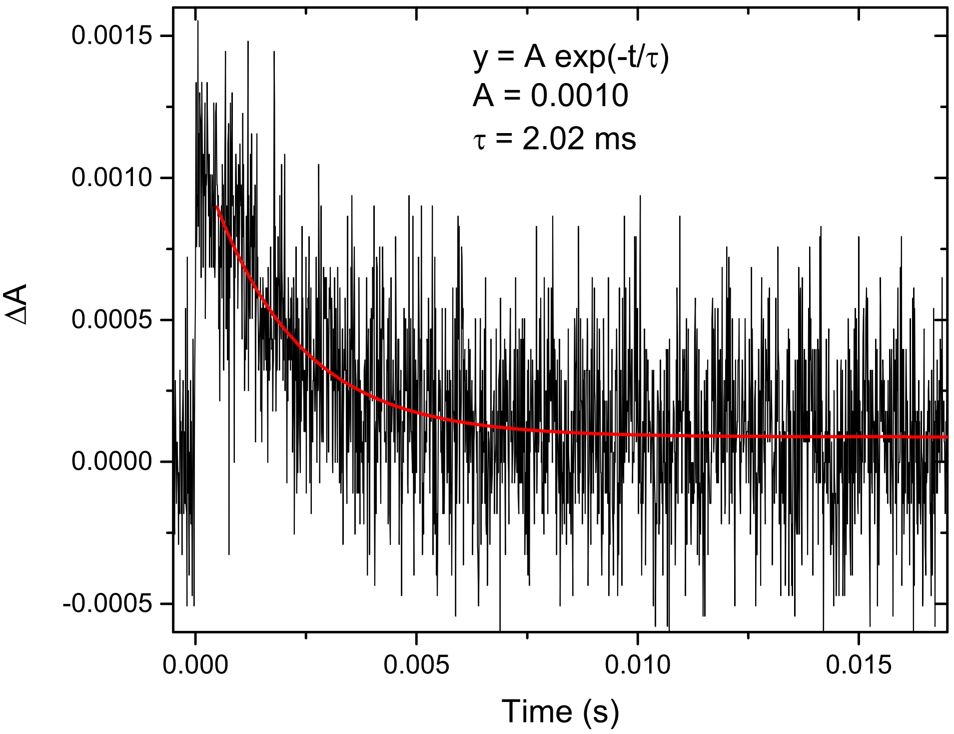

Figure S9: Transient absorption of **2** (10 μM) at 490 nm corresponding to the triplet absorption after sensitization by ZnOEP 0.5 μM (black) and fitted monoexponential decay (red).

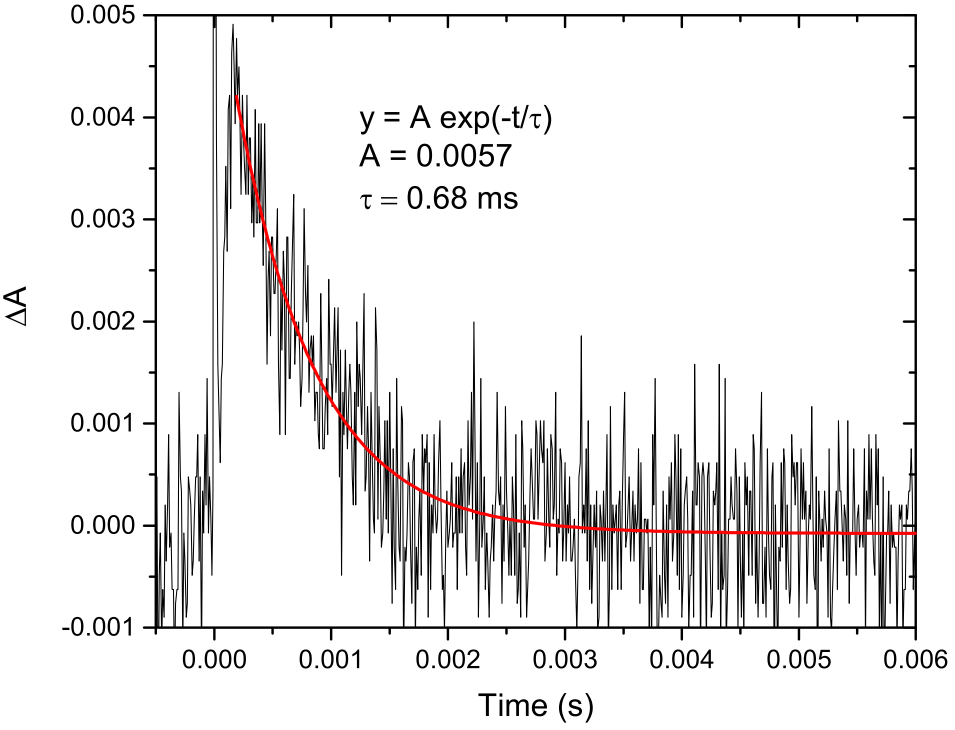

Figure S10: Transient absorption of **2** (10 μM) at 490 nm corresponding to the triplet absorption after sensitization by ZnOEP 50 μM (black) and fitted monoexponential decay (red).

5 DFT calculations

The results obtained using the B3LYP functional were compared to those using CAM-B3LYP. While CAM-B3LYP yields larger excitation energies as well as HOMO-LUMO energy differences, the qualitative results are very similar whence we conducted the majority of the analysis using only the B3LYP functional and exclusively present data obtained using the latter. We also considered the possibility of solvent induced changes in the absorption spectra using the universal solvation model introduced by Marenich *et al.*[S4] The resulting effects are, however, small, whence they were not explored any further.

The annihilator molecules were relaxed on both the S_0 and T_1 energy landscapes, in the latter case using an open shell DFT calculation. On the S_0 energy landscape the two thus obtained configurations are separated by 0.7 eV for all three molecules. Subsequently, the absorption spectra were computed for each of the resulting six configurations using TD-DFT starting from the singlet (S_0) wave function (Figure S11).

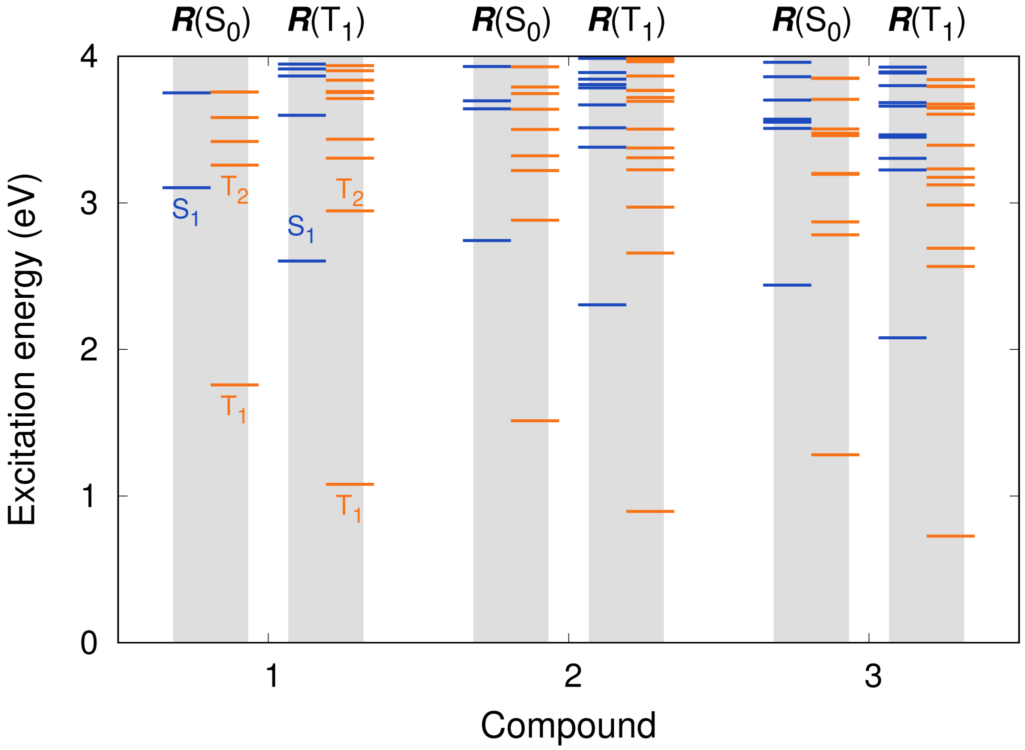

Figure S11: Calculated excitation spectra for configurations relaxed on the ground state singlet (R(S0)) and first triplet (R(T1)) landscape.

Furthermore, we studied the effect of phenyl group rotations on the excitation spectra.

To this end, the rotation angle of each phenyl group with respect to the central plane of the molecule was constrained, while the remaining degrees of freedom were allowed to fully relax on the T_1 potential energy surface (PES). Here, the T_1 PES was modeled by constraining the spin multiplicity in the DFT calculations to yield a triplet configuration. Subsequently, TDDFT calculations were carried out for each of the relaxed configurations based on the S_0 (ground state) wave function without allowing for any further relaxation. In these calculations the rotation angle of each phenyl group was constrained while allowing full relaxation of all other degrees of freedom. The two-dimensional range of rotation angles was sampled using a spacing of 15° and interpolated two a 1° grid for interpolation, Figure S12. For simplicity Figure 6 in the main text only displays the energies at $\Delta\theta_1 = -\Delta\theta_2$ from Figures S12A-G.

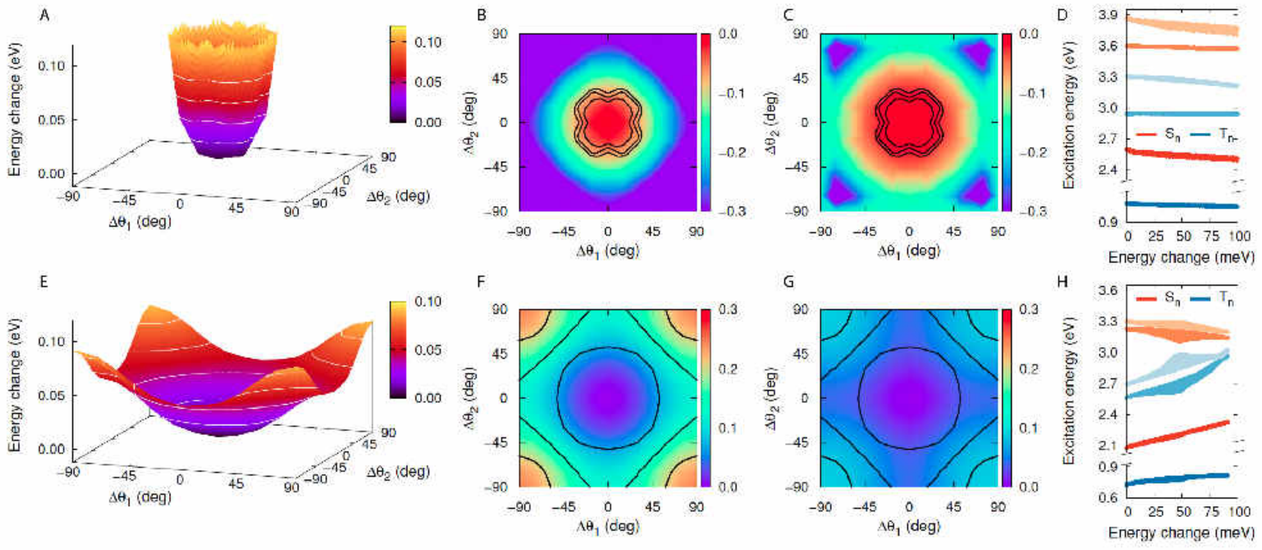

Figure S12: 2. Cross section of energy landscape for compounds A) **1** and E) **3** corresponding to rotation of the phenyl side groups away from the respective equilibrium angles ($\Delta\theta_1$,$\Delta\theta_2$). B,E) Variation of the excitation energy corresponding to the first singlet state (S1) in the same range of angles as in A and E. The black lines indicate changes in the total energy of the system corresponding to 25, 50, and 75 meV, respectively. C,G) As B and F but for the first triplet excitation (T1). D,H) Variation of both singlet (red, orange) and triplet (blue) excitations as a function of the energy relative to the ground state

6 Triplet-Triplet Annihilation

Transient absorption of the sensitizer and annihilator triplet, as well as the fluorescence of the upconverted annihilator singlet and sensitizer phosphorescence was monitored, using a ns-resolved transient absorption setup, to study the kinetics of the TTA-UC process. Transient absorption and emission with corresponding fits are displayed in figures S13-S15. In these figures the top graph shows the signal at 410 nm, 450 nm and 485 nm in blue for **1**, **2** and **3**, respectively. At these wavelengths the initial positive feature corresponds to the annihilator and sensitizer triplet absorption. The long-lived negative feature corresponds to the delayed upconverted fluorescence. The black signal is the sensitizer phosphorescence at 650 nm. Fits were done globally for both signals according to the procedures in reference S3[S3], the inset shows the first 5 μs. The fitting parameters k_{TTA}, k_{TET}, ϵ_{ET} and ϵ_{ST} are shown in each figure and are; the rate constant for triplet-triplet annihilation, the rate constant for triplet energy transfer, the annihilator triplet absorption coefficient and sensitizer triplet absorption coefficient, respectively.

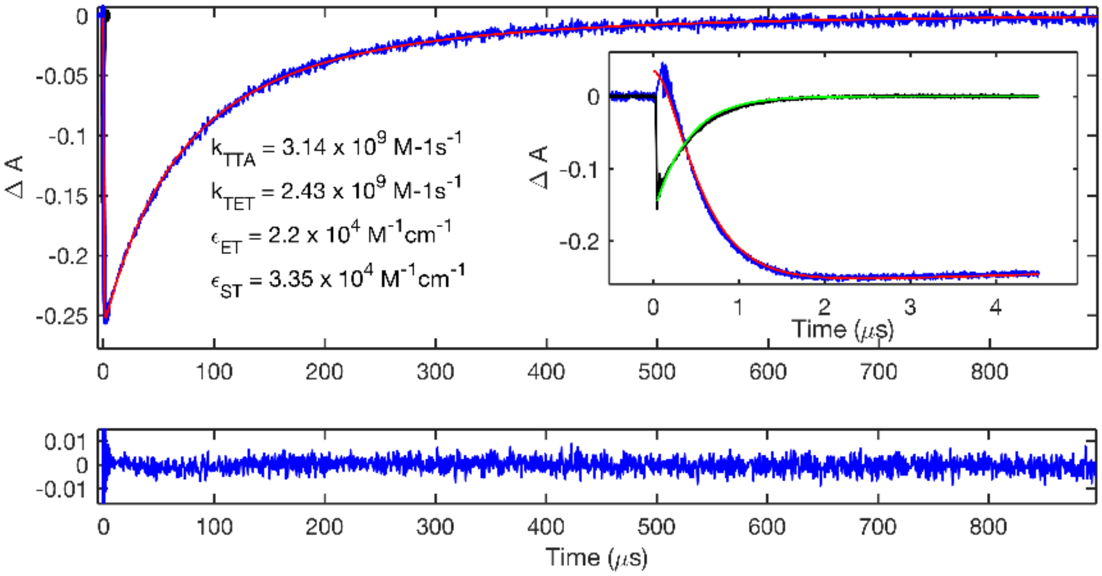

Figure S13: Transient absorption measurements of **1**(1 mM) and **PtOEP**(3.5μM) at 410 nm (blue) and 650 nm (black) and respective fits in red and green. Bottom panel shows the residual of the fitted annihilator decay.

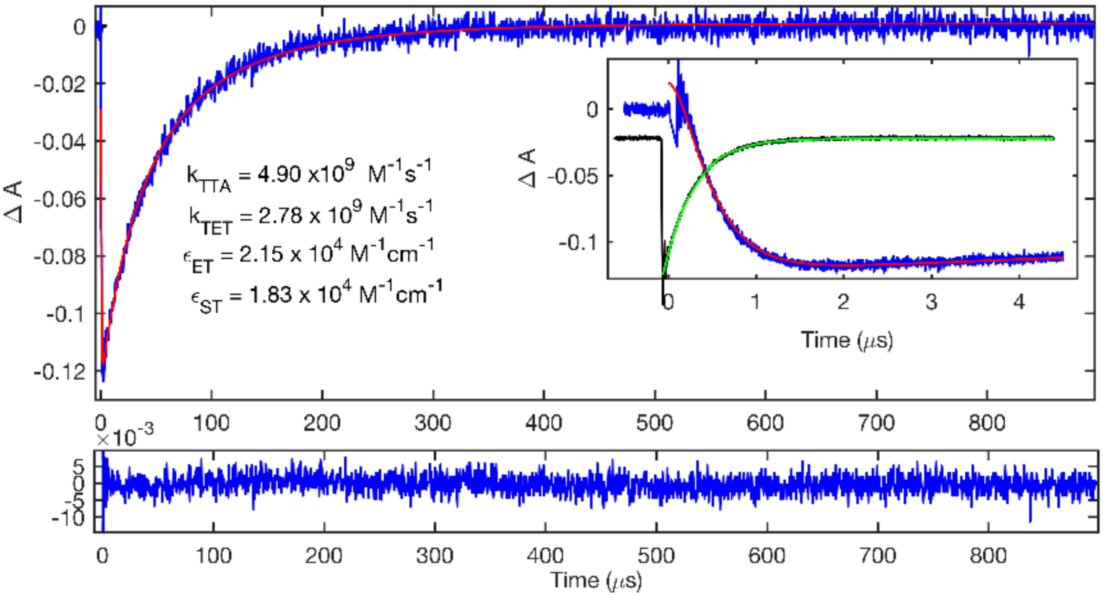

Figure S14: Transient absorption measurements of **2**(1 mM) and **PtOEP**(3.5μM) at 450 nm (blue) and 650 nm (black) and respective fits in red and green. Bottom panel shows the residual of the fitted annihilator decay.

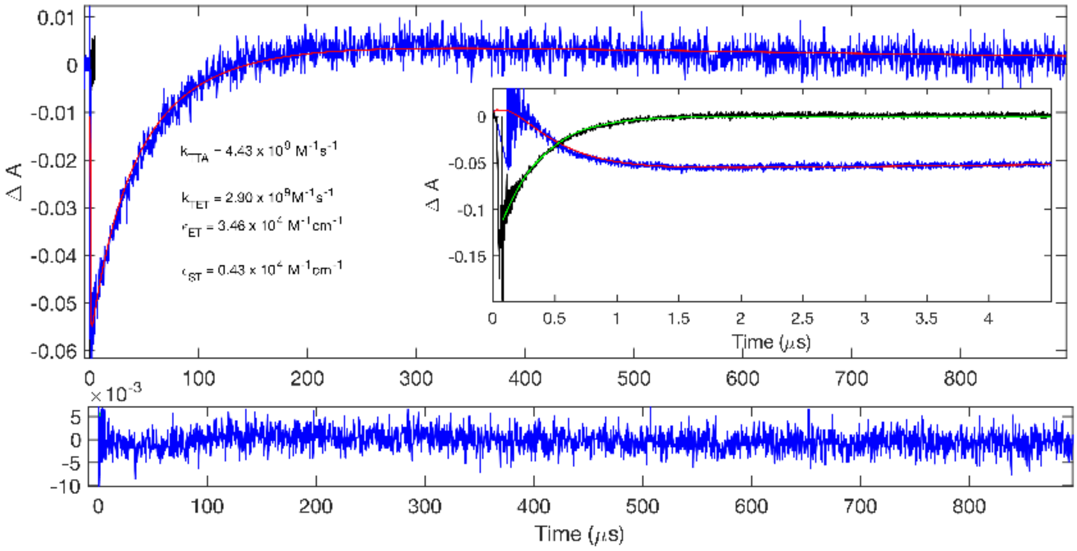

Figure S15: Transient absorption measurements of **3** (1 mM) and **PtOEP** (3.5μM) at 485 nm (blue) and 650 nm (black) and respective fits in red and green. Bottom panel shows the residual of the fitted annihilator decay

7 Rate-Equations for Triplet-Triplet Annihilation

Assuming that that the sensitizer concentration is low enough that no triplet-triplet annihilation occurs between sensitizer molecules or sensitizer and annihilator molecules, that the inter system crossing rate is fast and can be considered to be instantaneous the rate equations governing the triplet-triplet annihilation system are[S5]:

$$\frac{d[^1S]}{dt} = -k_{EX}[^1S]\Phi_{ISC} + k_{TET}[^3S^*][^1A] + k_{PS}[^3S^*] \tag{S3}$$

$$\frac{d[^3S^*]}{dt} = k_{EX}[^1S]\Phi_{ISC} - k_{TET}[^3S^*][^1A] - k_{PS}[^3S^*] \tag{S4}$$

$$\frac{d[^3A^*]}{dt} = k_{TET}[^3S^*][^1A] - 2k_{TTA}[^3A^*]^2 - k_{PA}[^3A^*] \tag{S5}$$

$$\frac{d[^1A^*]}{dt} = k_{TTA}[^3A^*]^2 - k_F[^1A^*] \tag{S6}$$

$$\frac{d[^1A]}{dt} = -k_{TET}[^3S^*][^1A] + k_{TTA}[^3A^*]^2 + k_F[^1A^*] \tag{S7}$$

where $[^3S^*]$ and $[^3A^*]$ are the sensitizer and annihilator triplet concentrations respectively. Correspondingly $[^1A^*]$ and $[^1A]$ are the concentrations of annihilator in the excited singlet and ground state respectively. k_{PA} and k_{PS} are the rate constants of triplet decay for the annihilator and sensitizer respectively. k_{EX} is the rate of excitation and is calculated from the absorption cross section of the sensitizer, α, in cm^2 and the photon flux, P, in photons/(s cm^2) according to Equation S8.

$$k_{EX} = \alpha P \tag{S8}$$

As described previously the triplet-triplet annihilation efficiency Φ_{TTA} can be determined from Equation S9 when assuming steady-state conditions.[S5]

$$\Phi_{TTA} = \frac{k_{TTA}[^3A^*]}{2k_{TTA}[^3A^*] + k_{PA}} \tag{S9}$$

Solving equations 3-7 with steady state conditions and using the maximum measured excitation intensity of 2600 mW/cm^2 at 532 nm used in our experiments, we can determine $[^3A^*]$ and consequently Φ_{TTA}. The obtained efficiencies are listed in Table S2.

Table S2: Calculated TTA efficiencies Φ_{TTA} and provisional spin-factor f.

Molecule	Φ_{TTA} (ZnOEP)	Φ_{TTA} (PtOEP)	f (ZnOEP)	f (PtOEP)
1	50%	50%	0.34	0.28
2	49%	49%	0.46	0.31
3	46%	48%	0.056	0.050

Assuming Φ_{ISC} of 1.0 and 0.9 for PtOEP and ZnOEP respectively, and Φ_{TET} of 1 according to figure S5 a spin-factor for the systems can be calculated from Equation S10 and they are listed in Table S2

$$\Phi_{UC} = f\Phi_{ISC}\Phi_{TET}\Phi_{TTA}\Phi_{AF} \tag{S10}$$

References

(S1) Börjesson, K.; Gilbert, M.; Dzebo, D.; Albinsson, B.; Moth-Poulsen, K. *RSC Adv.* **2014**, *4*, 19846.

(S2) Berlman, I. *Handbook of Fluorescence Spectra of Aromatic Molecules*, 2nd ed.; Academic Press: New York and London, 1971.

(S3) Gray, V.; Dzebo, D.; Lundin, A.; Alborzpour, J.; Abrahamsson, M.; Albinsson, B.; Moth-Poulsen, K. *J. Mater. Chem. C* **2015**, *3*, 11111–11121.

(S4) Marenich, A. V.; Cramer, C. J.; Truhlar, D. G. *J. Phys. Chem. B* **2009**, *113*, 6378–6396.

(S5) Gray, V.; Dzebo, D.; Abrahamsson, M.; Albinsson, B.; Moth-Poulsen, K. *Phys. Chem. Chem. Phys.* **2014**, *16*, 10345–52.